

Robust control of a quadcopter using PID and H_∞ controller

S. Madi^{1,*}, M. S. Larabi², N. M. Kherief³

¹Mechanical and Materials Engineering Laboratory (LGMM), University of August 20, 1955, Skikda, Algeria

²Automatic Laboratory, University of August 20, 1955, Skikda, Algeria

³Normal High School of Technology Education, University of August 20, 1955, Skikda, Algeria

ARTICLE INFO

Article Type:

Selected Article^c

Article History:

Received: 25 January 2023

Revised: 25 March 2023

Accepted: 12 April 2023

Published: 30 May 2023

Editor of the Article:

M. E. Şahin

Keywords:

PID control synthesis, Robust H_∞ controller, Quadcopter systems, Pitch angle, Roll angle, Yaw angle

ABSTRACT

In this article, two control units, the proportional integral derivative (PID) and robust H_∞ controller, are designed for controlling a quadcopter. The drone is a multi-input multi-output (MIMO) system whose control requires a lot of precision and durability. The objective of the control system is to ensure the tracking of the desired trajectory with precision in the face of the exogenous inputs (disturbance) which can affect the correct operation of the quad-copter. Support for harsh operating conditions due to model uncertainties that cause errors during operation. For this reason, controlling quad-copters is considered difficult and complex, which requires a compact and robust design. In this research we will study the design of a robust H_∞ controller based on optimal control, this technique is widely used in the control of multivariable systems. Then the robust H_∞ controller obtained is compared with a PID controller to justify the robustness of the H_∞ controller and the efficiency of the behaviour of the quad-copter with H_∞ concerning disturbances. The results of the simulation using MATLAB/Simulink showed the effectiveness of the method with acceptable trajectory tracking.

Cite this article: S. Madi, M. S. Larabi, N. M. Kherief, "Robust control of a quadcopter using PID and H_∞ controller," *Turkish Journal of Electromechanics & Energy*, 8(1), pp:3-11, 2023.

1. INTRODUCTION

In recent times, there have been significant technological advancements that have led to the emergence of drones that possess greater efficiency and are capable of carrying out a wide range of tasks, both in the civil and military sectors. These tasks include but are not limited to rescue operations, news coverage, climate monitoring, reconnaissance, and transportation missions [1]. However, it is worth noting that designing drones requires a high level of expertise. Unmanned Aerial Vehicles (UAVs) have the potential to replace manned vehicles in several dangerous missions, thereby reducing the prohibitive cost of air operations [2-4]. Achieving control of miniature rotary planes requires the integration of various fields, including control of the rotating vehicle and coordination control, among others [5].

Many studies have been performed on quadcopters using PID controllers modelled on [6], and there is a vast body of literature available in this area. In a particular study [7, 8], a simulation of pitch and roll moments for the quadcopter was achieved using both PID and PD controllers. H_∞ was used in [9] and [10] studies, which were very stimulating.

This study aims to compare two different quadcopter control methods, namely PID and H_∞ control, for controlling the yaw and

pitch channels under excursions and gusting conditions [11]. Determine the advantages and disadvantages of each control technique moreover to identify the most appropriate technique for the given conditions. The novelty of this work lies in the detailed comparison of the two control techniques and the selection of appropriate parameters and control settings. Several linear and nonlinear control technologies have achieved success in quadcopter control, such as PID controller, back-control, adaptive control, and H_∞ control [12, 13]. The PID controller is one of the most popular methods for quadcopter control due to its ease of use and simplicity. It can be easily set manually without requiring much experience, and it does not require a model of the system to be controlled [14, 15]. Moreover, the results are promising in dealing with potential disturbances and uncertainties [16].

To compare the two control techniques, a simulation model was created using MATLAB/Simulink. The model included a pitch and yaw system with excursions and gusting conditions. The PID control and H_∞ control were applied to the pitch and yaw channels separately. The novelty of this work lies in the detailed comparison of the two control techniques and the selection of appropriate parameters and control settings for H_∞ control.

^cInitial version of this article was presented at the 4th International Conference on Electromechanical Engineering (ICEE'2022) held on November 22-23, 2022, in Skikda, Algeria. It was subjected to a peer-review process before its publication.

*Corresponding author e-mail: s.madi@univ-skikda.dz

This study contributes to the existing literature by providing a comprehensive analysis of the advantages and disadvantages of two control techniques: PID and H^∞ control. The study focuses on the control of the Yaw and Pitch channels of a quadcopter under excursion and gusting conditions. Some advantages and disadvantages of both methods are summarized in Table 1.

Table 1. Comparative table of pros and cons of PID and H^∞ control.

Control Technique	Advantages	Disadvantages
PID Control	Simple and easy to implement	Susceptible to noise and disturbances
	Affordable and widely used	Limited in handling complex systems
	Tuning is easy	Non-linear systems may be difficult to control
H^∞ Control	Good for low and medium-bandwidth systems	May not be suitable for high-bandwidth systems
	Robust and effective for complex systems	Difficult to implement and requires advanced knowledge
	Can handle nonlinear systems	Expensive and time-consuming
	Resistant to disturbances and noise	Difficult to tune and requires expertise
	Provides a guaranteed level of performance	This may lead to over-conservative designs

2. PROPOSED SYSTEM MODEL

2.1. System Description

The quadcopter is controlled through four fundamental modes, namely vertical control, roll control, gradient control, and yaw control. Vertical flight control aims to manage the aircraft's ascent, descent, and take-off in the vertical direction by increasing or decreasing the speed of the four rotating propellers simultaneously. When the quadcopter is in a horizontal position, the inertial coordinate system synchronizes with the body coordinate system [17]. Two diagonal motors 1 and 3 are rotated in the same direction anti-clockwise whereas the others 2 and 4 in the clockwise direction to eliminate the anti-torque. Yaw angle is obtained by speeding up the clockwise motors or slowing down depending on the desired angle direction. Tilting around the x-roll angle axis allows the Quadcopter to move toward the y direction. Tilting around the y pitch angle axis allows the Quadcopter to move toward the x direction [18-21].

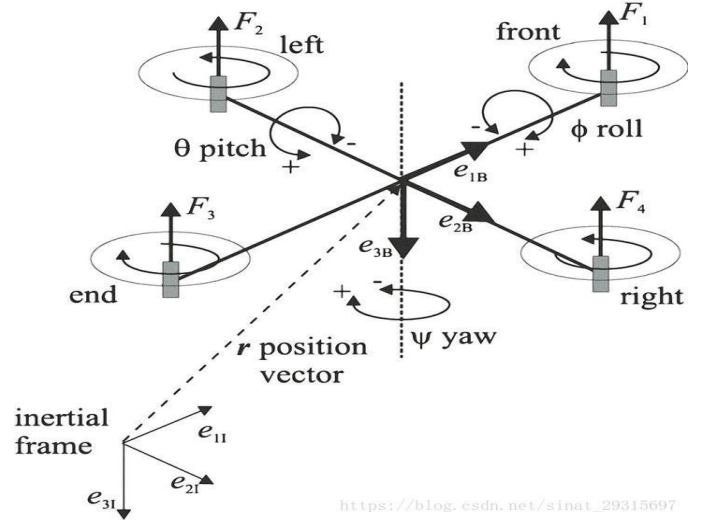


Fig. 1. Fixed and moving to coordinate sentences [22].

2.2. Quad Copter Modeling

The following equations can be used to express the relationship between the four fans' rotating speeds [23, 24].

$$\begin{cases} U1 = b(\Omega_1^2 + \Omega_2^2 + \Omega_3^2 + \Omega_4^2) \\ U2 = bl(\Omega_4^2 - \Omega_2^2) \\ U3 = bl(\Omega_3^2 - \Omega_1^2) \\ U4 = d(\Omega_2^2 - \Omega_1^2 + \Omega_4^2 - \Omega_3^2) \end{cases} \quad (1)$$

Where: Ω is the propeller speed, $U1$ thrust, $U2$, $U3$, and $U4$ torque, b , d is the thrust and drag factors, respectively, and l is the distance between the axes of rotation of two opposing motors. Figure 2 shows the structure model in hovering conditions.

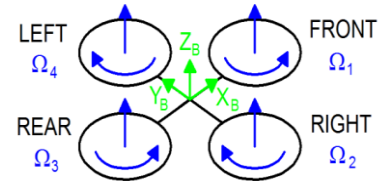


Fig. 2. Simplified quadcopter motor in hovering [25].

The rotation matrix about each of the coordinate axes is given in cartesian coordinates x , y & z , to simplify the equations, we set: $s\theta = \sin\theta$, $c\theta = \cos\theta$, $s\phi = \sin\phi$, $c\phi = \cos\phi$, $s\psi = \sin\psi$, $c\psi = \cos\psi$

- Roll ϕ is rotation around the x-axis
- Pitch θ is rotation around the y axis
- Yaw ψ is rotation around the z-axis

$$R(x, \phi) = \begin{bmatrix} 1 & 0 & 0 \\ 0 & c\phi & -s\phi \\ 0 & s\phi & c\phi \end{bmatrix} \quad (2)$$

$$R(y, \theta) = \begin{bmatrix} c\theta & 0 & s\theta \\ 0 & 1 & 0 \\ -s\theta & 0 & c\theta \end{bmatrix} \quad (3)$$

$$R(z, \psi) = \begin{bmatrix} c\psi & -s\psi & 0 \\ s\psi & c\psi & 0 \\ 0 & 0 & 1 \end{bmatrix} \quad (4)$$

The matrix of the total transformation between two coordinate clauses [26, 27].

$${}^B R_A = (\phi, \theta, \psi) = R(x, \phi). R(y, \theta). R(z, \psi) \quad (5)$$

$${}^B R_A = \begin{bmatrix} c\psi c\theta & s\psi s\theta c\psi - c\psi s\psi & c\psi s\theta c\psi + s\psi s\psi \\ s\psi c\theta & s\psi s\theta s\psi + c\psi c\psi & c\psi s\theta s\psi - s\psi c\psi \\ -s\theta & s\phi c\theta & c\phi c\theta \end{bmatrix} \quad (6)$$

Applying Newton's law of motion.

$$F = m\dot{V} + \Omega . m\vec{V} \quad (7)$$

$$T = I\dot{\Omega} + \Omega . I\vec{\Omega} \quad (8)$$

$$m\dot{V} = -mG + {}^B R_A F - F_A - \Omega . m\vec{V} \quad (9)$$

Where: V , m , ${}^B R_A$, F and $\Omega = [p \ q \ r]^T$ are linear velocity vector, quadcopter mass, transfer matrix and lifting force vector and the angular velocity vector respectively. Equation (10) determines linear acceleration based on factors such as mass, aerodynamic forces, propulsion forces, and angular velocities. Equation (11) details the correlation between the motor's angular velocities and the quadcopter's rotational velocities around the three axes while accounting for the effects of moments of inertia and gyroscopic forces. Equation (12) establishes a connection between the Euler angles and linear accelerations, taking into consideration factors such as gravity, aerodynamic forces, propulsion forces, and angular velocities.

$$m \begin{bmatrix} \ddot{x} \\ \ddot{y} \\ \ddot{z} \end{bmatrix} = -m \begin{bmatrix} 0 \\ 0 \\ g \end{bmatrix} + {}^B R_A \begin{bmatrix} 0 \\ 0 \\ U_1 \end{bmatrix} - \frac{1}{m} \begin{bmatrix} F_{Ax} \\ F_{Ay} \\ F_{Az} \end{bmatrix} - \begin{bmatrix} p \\ q \\ r \end{bmatrix} . m \begin{bmatrix} \dot{x} \\ \dot{y} \\ \dot{z} \end{bmatrix} \quad (10)$$

$$\begin{bmatrix} p \\ q \\ r \end{bmatrix} . m \begin{bmatrix} \dot{x} \\ \dot{y} \\ \dot{z} \end{bmatrix} = \begin{bmatrix} 0 & -r & q \\ r & 0 & -p \\ -q & p & 0 \end{bmatrix} . \begin{bmatrix} m\dot{x} \\ m\dot{y} \\ m\dot{z} \end{bmatrix} \quad (11)$$

$$\begin{cases} \ddot{x} = (c\psi s\theta c\psi + s\psi s\psi) \frac{U_1}{m} - \frac{F_{Ax}}{m} + q\dot{z} - r\dot{y} \\ \ddot{y} = (c\psi s\theta s\psi - s\psi c\psi) \frac{U_1}{m} - \frac{F_{Ay}}{m} + r\dot{x} - p\dot{z} \\ \ddot{z} = (c\psi c\theta) \frac{U_1}{m} - g - \frac{F_{Az}}{m} + q\dot{x} - r\dot{y} \end{cases} \quad (12)$$

The force of the four propellers is given by:

$$U_1 = f_1 + f_2 + f_3 + f_4 \quad (13)$$

Where f_i the thrust generated by the propeller i is equal to $f_i = b\Omega_i$ and b is the thrust constant.

$$I\dot{\Omega} = \tau + \tau_g - \Omega . I\vec{\Omega} \quad (14)$$

Where I , τ , and τ_g are: the plane inertia matrix, quad-copter propeller torque vector, and the gyroscopic torque due to a change in the direction of the plane of rotation of the propellers respectively.

$$\Omega = [p \ q \ r]^T \quad (15)$$

$$\begin{bmatrix} p \\ q \\ r \end{bmatrix} . \begin{bmatrix} I_{xx} & 0 & 0 \\ 0 & I_{yy} & 0 \\ 0 & 0 & I_{zz} \end{bmatrix} = \begin{bmatrix} p(I_{yy} - I_{zz}) \\ q(I_{zz} - I_{xx}) \\ r(I_{xx} - I_{yy}) \end{bmatrix} \quad (16)$$

Where

I_{xx} The moment of inertia for the x-axis

I_{yy} The moment of inertia for the y-axis

I_{zz} The moment of inertia for the z-axis

The angular motion equations are:

$$\dot{p} = (I_{yy} - I_{zz}) \frac{qr}{I_{xx}} + l \frac{\tau_\phi}{I_{xx}} + \frac{I_r \Omega_r}{I_{xx}} \dot{q} \quad (17)$$

$$\dot{q} = (I_{zz} - I_{xx}) \frac{pr}{I_{yy}} + l \frac{\tau_\theta}{I_{yy}} + \frac{I_r \Omega_r}{I_{yy}} \dot{p} \quad (18)$$

$$\dot{r} = (I_{xx} - I_{yy}) \frac{pq}{I_{zz}} + l \frac{\tau_\psi}{I_{zz}} \quad (19)$$

$$\tau_\phi = l(f_4 - f_2) \quad (20)$$

$$\tau_\theta = l(f_3 - f_1) \quad (21)$$

$$\tau_\psi = T_1 - T_2 + T_3 - T_4 \quad (22)$$

$$T = d\Omega^2 \quad (23)$$

Therefore, the equations of total motion are:

$$\begin{cases} \ddot{x} = (c\psi s\theta c\psi + s\psi s\psi) \frac{U_1}{m} - \frac{F_{Ax}}{m} + q\dot{z} - r\dot{y} \\ \ddot{y} = (c\psi s\theta s\psi - s\psi c\psi) \frac{U_1}{m} - \frac{F_{Ay}}{m} + r\dot{x} - p\dot{z} \\ \ddot{z} = (c\psi c\theta) \frac{U_1}{m} - g - \frac{F_{Az}}{m} + q\dot{x} - r\dot{y} \end{cases} \quad (24)$$

$$\dot{p} = (I_{yy} - I_{zz}) \frac{qr}{I_{xx}} + l \frac{\tau_\phi}{I_{xx}} + \frac{I_r \Omega_r}{I_{xx}} \dot{q} \quad (25)$$

$$\dot{q} = (I_{zz} - I_{xx}) \frac{pr}{I_{yy}} + l \frac{\tau_\theta}{I_{yy}} + \frac{I_r \Omega_r}{I_{yy}} \dot{p} \quad (26)$$

$$\dot{r} = (I_{xx} - I_{yy}) \frac{pq}{I_{zz}} + l \frac{\tau_\psi}{I_{zz}} \quad (27)$$

The characteristics of the quadcopter used in this study are shown in Table 2.

Table 2. Quad-copter parameters [28].

Symbol	Name	Value	Unit
m	Quadcopter mass	0.65	Kg
I_{xx}	Moment of inertia on the X axis	0.0075	Kg.m ²
I_{yy}	Moment of inertia on the Y axis	0.0075	Kg.m ²
I_{zz}	Moment of inertia on the Z axis	0.013	Kg.m ²
b	Thrust Coefficient	3.3*10 ⁻⁵	N. s ²
d	Drag Coefficient	7.5*10 ⁻⁵	N.m.s ²
l	Length of a quadcopter	0.23	m
g	Gravity	9.81	m/s ²

3. PID CONTROLLER DESING

A proportional integral derivative (PID) is a controller widely used in regulation for its simplicity of adjustment. it corrects the servo error so that the output follows perfectly the variations of the input with the improvement of the performances and the robustness of the looped system, that is to say, the system must be stable, fast and precise in a closed loop whatever the uncertain model [16, 29-31]. The block diagram of a generic closed-loop control system with the PID controller is illustrated in Figure 3.

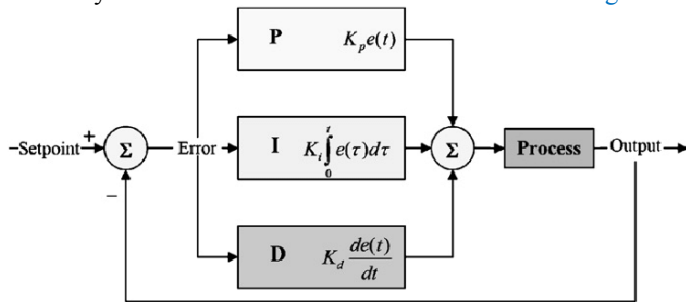


Fig. 3. PID controller in a feedback loop.

The transfer function of the PID controller is r as shown in equation (28). [32]

$$PID(s) = \frac{K_d s^2 + K_p s + K_i}{s} \quad (28)$$

K_p , K_i and K_d are the proportional, integral and derivative gains.

The mathematical expression (29) of the PID controller is used to regulate an output variable (u) according to the error between the setpoint value (r) and the measurement variable (y).

$$u = K_p e + K_i \int e dt + K_d \frac{d}{dt} e \quad (29)$$

Each of these characteristics can be modified to improve control efficiency. Therefore, each axis of the drone must be assigned a value for K_p , K_i , and K_d . So that the PID controller is created for the three angles of the quad-copter ϕ Roll, θ pitch, and ψ yaw. The quad-copter that appears to be more sensitive and responsive to angle change increases with increasing relative gain factor. The quad-copter will appear slow and be challenging to control if it is too low. When the P gain is too high, you might notice that the quadcopter begins to oscillate at a high frequency. when there are irregular winds, The angular position's precision may be improved by the integrated gain factor; but if the I value becomes too high, the quad-copter may begin to react slowly and have lower relative gains; as a result, it may also begin to oscillation as though it were experiencing high P gains but at a lower frequency.

The actions of the gains of the PID regulator have the following effects:

A proportional controller with K_p reduces rise time and tracking error, but it cannot eliminate steady-state error. Adding the integral gain K_i can eliminate the steady-state error, but it may negatively affect the transient response. On the other hand, the derivative gain K_d increases system stability reduces overshoot, and improves transient response. However, it can amplify measurement noise.

4. SIMULATIONS RESULTS WITH PID CONTROLLER

Figure 4 (a-d) appear the results of different PID controllers for attitude stabilization in terms of their proportional, integral, and derivative responses. Each controller demonstrates varying levels of correction for altitude, roll angle, pitch angle, and yaw angle errors. These findings provide insights into the performance of PID control in quadcopters and can guide future optimization and tuning of controller parameters.

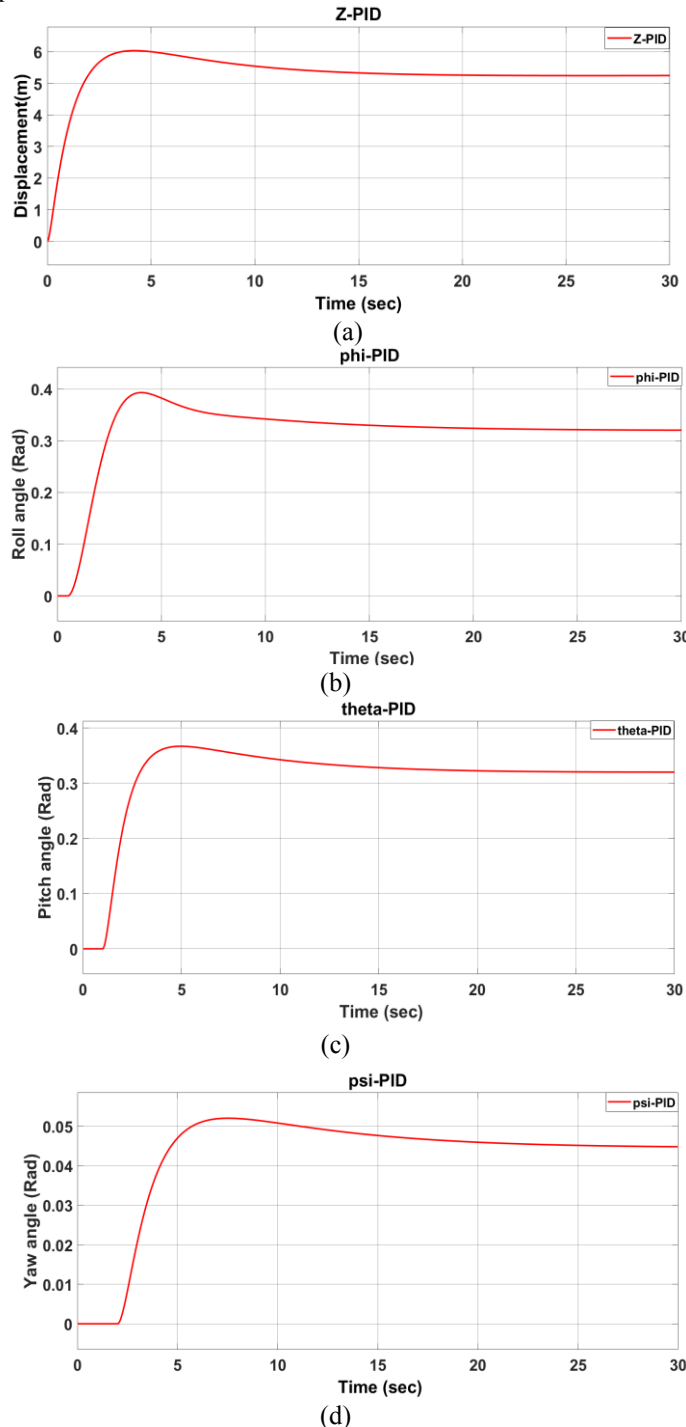


Fig.4. Step responses with PID controller: (a) Z displacement, (b) Roll angle (phi), (c) The pitch angle (theta), (d) Yaw angle (psi).

5. H ∞ CONTROLLER DESIGN

The H ∞ controller is a robust linear controller, whose design is based on static or dynamic feedback control in which input and output weighting functions are specified to achieve robustness and performance requirements, which can be modified to reach the robust design of the controller [10, 17, 33-36].

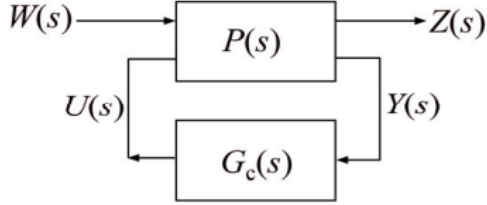


Fig. 5. H ∞ standard block diagram.

The following state space (30) is obtained by manipulating the equations in section 2.2, which describe the modelling of the quadcopter:

$$\begin{cases} \dot{x} = A(t)x(t) + B(t)u(t) \\ y = C(t)x(t) + D(t)u(t) \end{cases} \quad (30)$$

Where: $x = [\varphi \ \dot{\varphi} \ \theta \ \dot{\theta} \ \psi \ \dot{\psi} \ Z \ \dot{Z}]^T \in \mathfrak{R}^n$ is the system state vector, $u(t) = [U_1 \ U_2 \ U_3 \ U_4]^T \in \mathfrak{R}^l$ is the control vector, and $y(t) = [\varphi \ \theta \ \psi \ Z]^T \in \mathfrak{R}^m$ is the output vector, with:

$$A = \begin{bmatrix} 0 & 1 & 0 & 0 & 0 & 0 & 0 & 0 \\ 0 & 0 & 0 & 0 & 0 & 0 & 0 & 0 \\ 0 & 0 & 0 & 1 & 0 & 0 & 0 & 0 \\ 0 & 0 & 0 & 0 & 0 & 0 & 0 & 0 \\ 0 & 0 & 0 & 0 & 0 & 1 & 0 & 0 \\ 0 & 0 & 0 & 0 & 0 & 0 & 0 & 0 \\ 0 & 0 & 0 & 0 & 0 & 0 & 0 & 1 \\ 0 & 0 & 0 & 0 & 0 & 0 & 0 & 0 \end{bmatrix}, \quad B = \begin{bmatrix} 0 & 0 & 0 & 0 \\ \frac{1}{I_x} & 0 & 0 & 0 \\ 0 & 0 & 0 & 0 \\ 0 & \frac{1}{I_y} & 0 & 0 \\ 0 & 0 & 0 & 0 \\ 0 & 0 & \frac{1}{I_z} & 0 \\ 0 & 0 & 0 & 0 \\ 0 & 0 & 0 & \frac{1}{m} \end{bmatrix} = \begin{bmatrix} 0 & 0 & 0 & 0 \\ 133.3 & 0 & 0 & 0 \\ 0 & 0 & 0 & 0 \\ 0 & 133.3 & 0 & 0 \\ 0 & 0 & 0 & 0 \\ 0 & 0 & 76.92 & 0 \\ 0 & 0 & 0 & 0 \\ 0 & 0 & 0 & 1.538 \end{bmatrix},$$

$$C = \begin{bmatrix} 1 & 0 & 0 & 0 & 0 & 0 & 0 & 0 \\ 0 & 0 & 1 & 0 & 0 & 0 & 0 & 0 \\ 0 & 0 & 0 & 0 & 1 & 0 & 0 & 0 \\ 0 & 0 & 0 & 0 & 0 & 0 & 1 & 0 \end{bmatrix}, \quad D = \begin{bmatrix} 0 & 0 & 0 & 0 \\ 0 & 0 & 0 & 0 \\ 0 & 0 & 0 & 0 \\ 0 & 0 & 0 & 0 \end{bmatrix}.$$

The transfer matrix of the plant is given by:

$$G(s) = C(sI + A)^{-1}B + D = \begin{bmatrix} \frac{1}{s^2} & 0 & 0 & 0 \\ 0 & \frac{133.3}{s^2} & 0 & 0 \\ 0 & 0 & \frac{123.5}{s^2} & 0 \\ 0 & 0 & 0 & \frac{70.42}{s^2} \end{bmatrix} \quad (31)$$

The closed-loop block diagram of the system with H ∞ control is shown in Figure 6.

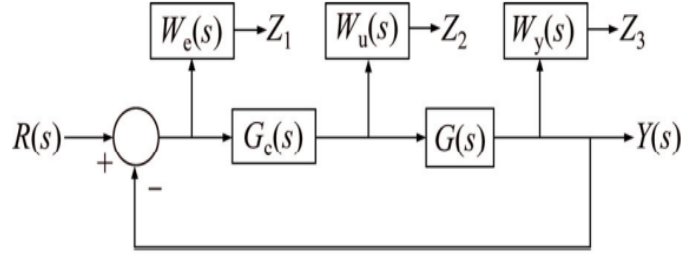


Fig. 6. H ∞ with loop shaping block diagram.

The state space model for the augmented plant can be described as follows [37]:

$$P(s) = \begin{bmatrix} P_{11} & P_{12} \\ P_{21} & P_{22} \end{bmatrix} = \begin{bmatrix} A & B_1 & B_2 \\ C_1 & D_{11} & D_{12} \\ C_2 & D_{21} & D_{22} \end{bmatrix} = \begin{bmatrix} W_e(s) & -W_e(s) \cdot G(s) \\ 0 & W_u(s) \\ 0 & W_y(s) \cdot G(s) \\ 1 & -G(s) \end{bmatrix} \quad (32)$$

$$F(P(s), G_e(s)) = P_{11} + P_{12} * G_e(s) * (1 - P_{22} * G_e(s))^{-1} * P_{21} \quad (33)$$

The weighting functions make it possible to obtain a robust Hinf controller which satisfies the conditions of robustness in stability and performance of the closed loop by minimizing. The mathematical condition in Equation (34) satisfies the stability of the transfer function in Equation (31)

$$\|F(P(s), G_e(s))\|_{\infty} = \left\| \begin{bmatrix} w_e * S(s) \\ w_u * K(s) \\ w_y * T(s) \end{bmatrix} \right\|_{\infty} < 1 \quad (34)$$

The following weighting functions w_e , w_u and w_y which are given in Equations (35), (36), (37) are obtained by using several repeated trial and error attempts until the optimization problem is successfully solved to achieve the control objectives in terms of stability and performance of the closed system.

$$w_e = \text{diag}$$

$$\left(\left[\frac{s^2 + 5.44s + 16}{(s + 5.437)(s + 0.002943)}, \frac{s^2 + 12.18s + 64.1}{(s + 0.005265)(s + 12.17)}, \frac{s^2 + 12.18s + 64.1}{(s + 0.005265)(s + 12.17)}, \frac{s^2 + 6.73s + 25}{(s + 0.003717)(s + 6.726)} \right] \right) \quad (35)$$

$$w_u = \text{diag}$$

$$([0.000625, 0.000625, 0.000625, 0.000625]) \quad (36)$$

$$w_y = \text{diag}$$

$$\left(\left[\frac{100*s + 640}{s + 8000}, \frac{100*s + 640}{s + 8000}, \frac{100*s + 640}{s + 8000}, \frac{100*s + 560}{s + 7000} \right] \right) \quad (37)$$

6. SIMULATIONS RESULTS WITH H^∞ CONTROLLER

Figures 7, 8, and 9 show the sensitivity and complementary sensitivity functions, it can be said that the system can reject disturbances and track reference inputs, and the control unit handles disturbances well.

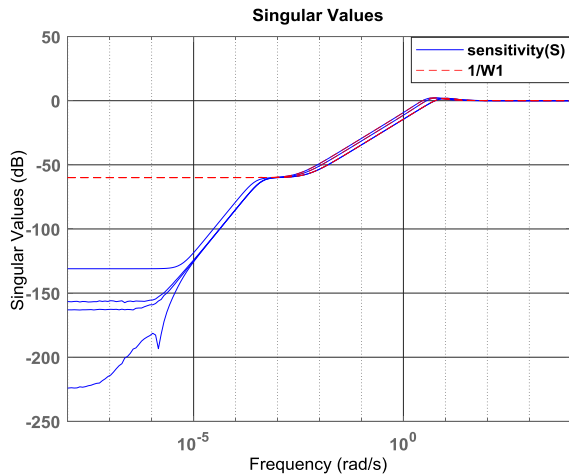


Fig. 7. Sensitivity (singular values).

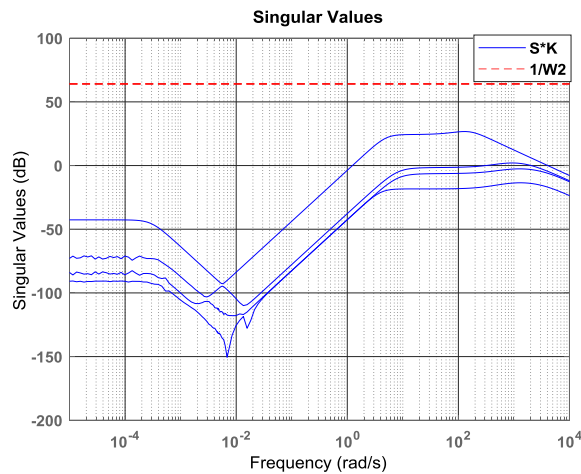


Fig. 8. Sensitivity ($S \cdot K$).

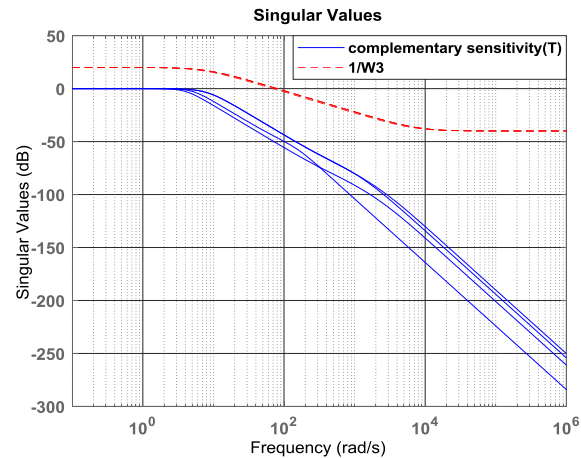
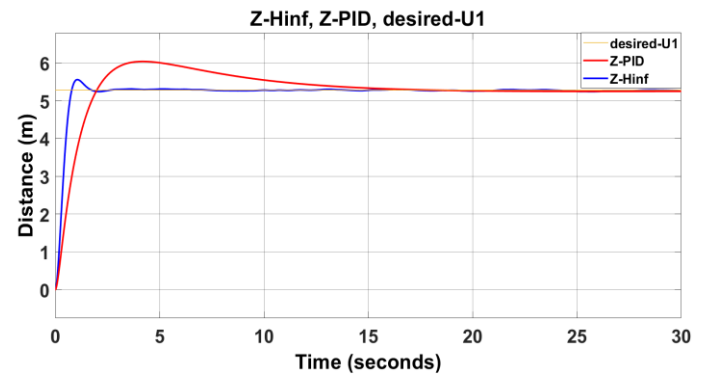


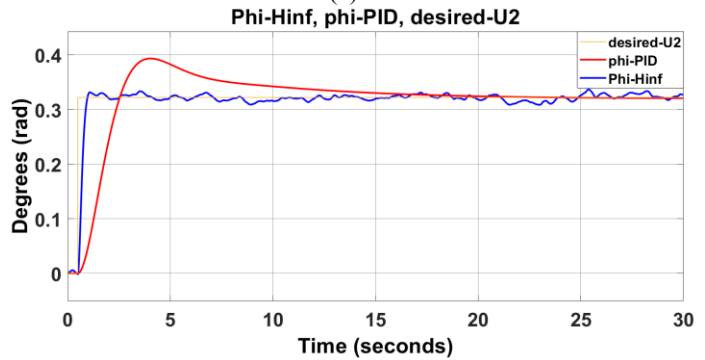
Fig. 9. Complementary sensitivity (singular values).

The results in Figure 10 (a-d) show that the H^∞ control technique outperforms the PID control technique in terms of both overshoot and rise time. H^∞ control exhibits lower

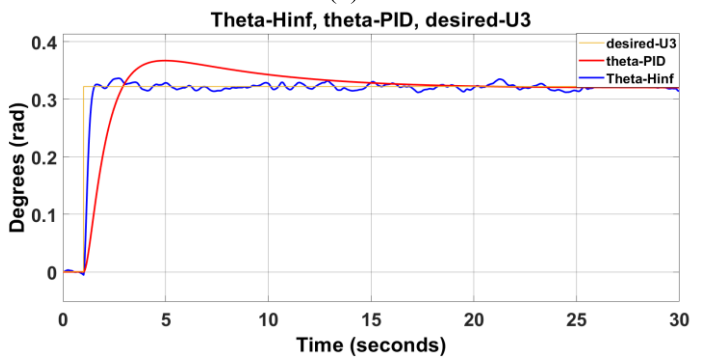
overshoot and faster rise time for all axes, indicating better stability and response speed compared to PID control. These findings highlight the effectiveness of H^∞ control for precise and efficient attitude stabilization in quadcopters.



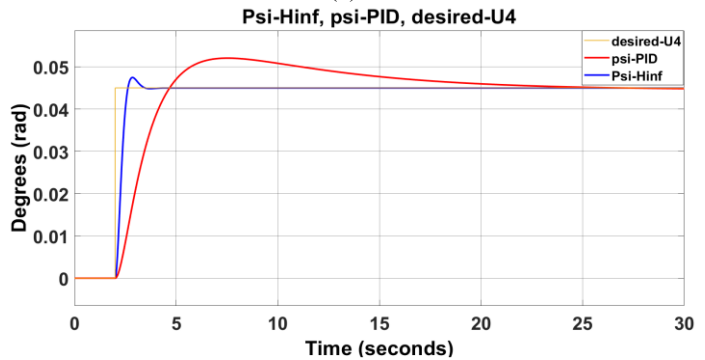
(a)



(b)



(c)



(d)

Fig. 10. Step responses with PID and H^∞ controller (comparison): (a) Z displacement, (b) Roll angle (ϕ), (c) Pitch angle (θ), (d) Yaw angle (ψ).

7. INTERPRETATIONS

The simulation results demonstrate that the PID controller effectively tracks the desired paths for the roll angle, tilt angle, skew angle, and offset based on the position command of the quadcopter, although there is a 20% overshoot and the response is slow which is considered acceptable. Therefore, it can be considered that the PID control has been successful in achieving stability for the system. In comparison, the H_∞ controller shows an impressive performance in reducing overshoot and response time. The response time of the quadcopter is considered real-time, which is an excellent outcome for the H_∞ controller. The singular values of the cost function indicate that the controller has all the desired characteristics that decrease at high frequencies, demonstrating the successful design of the controller.

The match between $S(s)$ and $1/W(s)$ is good at low frequencies, while $T(s)$ closely follows $1/W(s)$ at high frequencies. The simulation results confirm that the H_∞ controller is highly capable of rejecting low-frequency disturbances and attenuating high-frequency noise.

8. CONCLUSION

To evaluate the performance of the PID and H_∞ controller techniques in regulating the Yaw and Pitch channels of a quadcopter, we conducted simulations using MATLAB/Simulink. For both controllers, we used the same quadcopter model and initial conditions. We subjected the quadcopter to disturbances and gusting conditions and analyzed the performance of the controllers in terms of control errors and control effort. Our simulation results show that the H_∞ controller outperforms the PID controller in terms of robustness and stability. Specifically, the H_∞ controller was able to regulate the Yaw and Pitch channels with smaller control errors and a more stable response, even under adverse conditions. In contrast, the PID controller showed larger control errors and a less stable response under the same conditions. To further investigate the performance of the H_∞ controller we selected the control parameters and settings for the weightings matrices using linear H infinity. Specifically, we conducted sensitivity analysis and trade-off studies to select the most appropriate values for the weightings matrices. Our results show that the selected values resulted in a compact and robust design, with a satisfactory level of performance in terms of control errors and control effort. Overall, our study provides a valuable contribution to the existing body of knowledge in the field of quadcopter control. Our results demonstrate the superiority of the H_∞ controller over the PID controller in regulating the Yaw and Pitch channels of a quadcopter, especially under adverse conditions. Our selection of the control parameters and settings for the weightings matrices in the H_∞ controller using linear H_∞ provides a useful guideline for designing a robust control system for quadcopters and other MIMO systems.

Appendix

The Ziegler-Nichols closed-loop oscillation method is a common approach to tuning the parameters of a PID controller. The method is carried out in closed-loop mode, with the control action starting in proportional mode and the gain gradually increased until closed-loop oscillations occur for both the pitch,

roll, yaw and displacement. The period of these oscillations is used to calculate the optimal values for K_p , K_i , and K_d using a software tool called the Method Tuner. The recommended values for these parameters are presented in Table A.

Table A. PID parameters.

Control	PIDz	PIDphi	PIDteta	PIDpsi
P	0.0015151	0.1110491	0.0024138	0.065741
I	7.7383e-5	4.2104e-5	0.000113	0.0024117
D	0.007315	0.0062407	0.012661	0.43462

In the H_∞ controller, the selection of weighting matrices was based on the system characteristics and desired control performance. A diagonal weighting matrix was initially used with equal weights assigned to all states. The diagonal elements were then modified based on the significance of each state to the control objective. The iterative process was used to refine the weighting matrices until achieving the desired control performance while minimizing the control effort. The MATLAB robust control toolbox was used to simulate the closed-loop system response, evaluate system sensitivity to weighting matrix changes, and refine the weighting matrices to improve stability and performance. Table B provides a comparison of overshoot and rises time for the different control techniques.

Table B. Overshoot and rise time comparison.

Control Technique		Overshoot (%)	Rise Time (sec)
PID Control	Roll	22.840	1.382
	Thrust	15.698	1.351
	Yaw	15.698	1.835
	Pitch	14.368	1.295
H_∞ Control	Roll	2.677	0.293
	Thrust	5.851	0.509
	Yaw	5.851	0.406
	Pitch	1.547	0.300

These results are obtained after running the H_∞ optimization program which led to $\gamma = 1.0012$ in just a few iterations, which explains the robustness dilemma, ie any performance adjustment generates a stability adjustment.

Acknowledgement

We are grateful to Prof. Dr Kherief Nacereddine Mohamed for giving us advice and presenting the project to us in an easy to understand manner which helped us to complete our project easily and effectively on time. We are deeply grateful to Dr Mohand Said Larabi for allowing us to work on this project which provided valuable information on the subject of robust control, thank you.

References

- [1] N. Michael, J. Fink, and V. Kumar, "Cooperative manipulation and transportation with aerial robots," *Autonomous Robots*, 30(1), pp. 73-86, 2011.
- [2] Z. Tahir, W. Tahir, and S. A. Liaqat, "State space system modelling of a quadcopter UAV," *arXiv preprint arXiv:1908.07401*, 2019.

- [3] C. C. Chen, and Y. T. Chen, "Feedback linearized optimal control design for a quadrotor with multi-performances," *IEEE Access*, vol. 9, pp. 26674-26695, 2021.
- [4] N. P. Nguyen, and S. K. Hong, "Sliding mode thau observer for actuator fault diagnosis of quadcopter UAVs," *Applied Sciences*, 8(10), pp. 1893, 2018.
- [5] S. Bouabdallah, and R. Siegwart, "Backstepping and sliding-mode techniques applied to an indoor micro quadrotor," *IEEE international conference on robotics and automation*, Barcelona, Spain, 2005, pp. 2247-2252.
- [6] M. Karahan, and C. Kasnakoglu, "Modeling and simulation of quadrotor UAV using PID controller," *11th ECAI Conferencance*, Pitesti, Romania, 2019, pp. 1-4.
- [7] G. T. Navajas, and S. R. Prada, "Building your own quadrotor: A mechatronics system design case study," *III. International Congress of Engineering Mechatronics and Automation*, Cartagena, Colombia, 2014, pp. 1-5.
- [8] V. Praveen, and S. Pillai, "Modeling and simulation of quadcopter using PID controller," *International Journal of Control Theory and Applications*, 9(15), pp. 7151-7158, 2016.
- [9] L. Abdou, "Integral backstepping/LFT-LPV H_∞ control for the trajectory tracking of a quadcopter," *7th International Conference on Systems and Control*, 2018, pp. 348-353.
- [10] C. Massé, O. Gougeon, D.-T. Nguyen and D. Saussié, "Modeling and control of a quadcopter flying in a wind field: A comparison between LQR and structured H_∞ control techniques," *International Conference on Unmanned Aircraft Systems (ICUAS)*, 2018, pp. 1408-1417.
- [11] M. De Freitas Virgilio Pereira, "Constrained Control for Load Alleviation in Very Flexible Aircraft," *PhD. Thesis, University of Michigan*, 2022.
- [12] Y. Naidoo, R. Stopforth, and G. Bright, "Quad-Rotor unmanned aerial vehicle helicopter modelling & control," *International Journal of Advanced Robotic Systems*, 8(4), pp. 45, 2011.
- [13] Z. M. Carlton, "System Identification and Verification of Rotorcraft UAVs," *Ph.D. Thesis, University of Cincinnati*, 2017.
- [14] P. Moonumca, Y. Yamamoto, and N. Depaiwa, "Adaptive PID for controlling a quadrotor in a virtual outdoor scenario: Simulation study," *International Conference on Mechatronics and Automation*, 2013, pp. 1080-1086.
- [15] S. Bouabdallah, A. Noth, and R. Siegwart, "PID vs LQ control techniques applied to an indoor micro quadrotor," *International Conference on Intelligent Robots and Systems*, 2004, pp. 2451-2456.
- [16] H. Bolandi, M. Rezaei, R. Mohsenipour et al., "Attitude control of a quadrotor with optimized PID controller," *Intelligent Control and Automation*, 4(3), pp. 335-342, 2013.
- [17] A. Noormohammadi-Asl, O. Esrafilian, M. A. Arzati et al., "System identification and H_∞ -based control of quadrotor attitude," *Mechanical Systems and Signal Processing*, vol. 135, pp. 106358, 2020.
- [18] B. J. Emran, "Globally robust tracking control of a quadrotor aerial vehicle for multi-behaviour applications," *PhD. Thesis, University Of British Columbia (Okanagan)*, 2019.
- [19] S. L. Rangajeeva, and J. F. Whidborne, "Linear parameter varying control of a quadrotor," *6th International Conference on Industrial and Information Systems*, 2011, pp. 483-488.
- [20] R. W. Beard, "Quadrotor dynamics and control," Brigham Young University, *Tech. Report*, vol. 19, pp. 46-56, 2008.
- [21] M. Kerma, A. Mokhtari, B. Abdelaziz et al., "Nonlinear H_∞ control of a quadrotor (UAV), using high order sliding mode disturbance estimator," *International Journal of Control*, 85(12), pp. 1876-1885, 2012.
- [22] A. Manjunath, P. Mehrok, R. Sharma et al., "Application of virtual target based guidance laws to path following of a quadrotor UAV," *International conference on unmanned aircraft systems (ICUAS)*, 2016, pp. 252-260.
- [23] C. Coza, C. Nicol, C. Macnab et al., "Adaptive fuzzy control for a quadrotor helicopter robust to wind buffeting," *Journal of Intelligent & Fuzzy Systems*, 22(5-6), pp. 267-283, 2011.
- [24] R. Guardado, M. J. López, and V. M. Sánchez, "MIMO PID controller tuning method for quadrotor based on LQR/LQG theory," *Robotics*, 8(2), pp. 36, 2019.
- [25] M. Manimaraboopathy, H. V. Christopher, and S. Vignesh, "Unmanned fire extinguisher using quadcopter," *International Journal on Smart Sensing and Intelligent Systems*, 10(5), pp. 471-481, 2017.
- [26] M. H. Guisser, and H. Medromi, "Commande robuste en temps discret d'un robot volant quadrirotor en présence de vent," *WOTIC'09 Conference*, Agadir, Morocco, December 2009.
- [27] Y. Chen, Y. He, and M. Zhou, "Modeling and control of a quadrotor helicopter system under impact of wind field," *Research Journal of Applied Sciences, Engineering and Technology*, 6(17), pp. 3214-3221, 2013.
- [28] L. Cedro, and K. Wieczorkowski, "Optimizing PID controller gains to model the performance of a quadcopter," *Transportation Research Procedia*, vol. 40, pp. 156-169, 2019.
- [29] B. Kamel, B. Yasmina, B. Laredj et al., "Dynamic modeling, simulation and PID controller of unmanned aerial vehicle UAV," *Seventh International Conference on Innovative Computing Technology (INTECH)*, 2017, pp. 64-69.
- [30] L. E. Romero, D. F. Pozo, and J. A. Rosales, "Quadcopter stabilization by using PID controllers," *Maskana*, vol. 5, pp. 175-186, 2014.
- [31] L. Zhou, A. Pljonkin, and P. K. Singh, "Modeling and PID control of quadrotor UAV based on machine learning," *Journal of Intelligent Systems*, 31(1), pp. 1112-1122, 2022.
- [32] R. Çelikel, M. Özdemir, and Ö. Aydoğmuş, "Implementation of a flywheel energy storage system for space applications," *Turkish Journal of Electrical Engineering and Computer Sciences*, 25(2), pp. 1197-1210, 2017.
- [33] A. G. Varghese, and D. Sreekala, "Modeling and design of UAV with LQG and H_∞ controllers," *International Journal of Engineering Research & Technology (IJERT)*, 8(5), pp. 446-450, 2019.
- [34] T. M. I. Hakim, and O. Arifianto, "Implementation of Dryden continuous turbulence model into Simulink for LSA-02 flight test simulation," *Journal of Physics: Conference Series*, IOP Publishing, 2018, pp. 012017.

[35] T. Kang, K. J. Yoon, T.-H. Ha and G. Lee "H-infinity control system design for a quad-rotor," *Journal of Institute of Control, Robotics and Systems*, 21(1), pp. 14-20, 2015.

[36] P. Priya, and S. S. Kamlu, "Robust Control Algorithm for Drones," *Aeronautics-New Advances: Intech Open Publ.*, 2022.

[37] A. Jafar, S. Fasih-UR-Rehman, S. Fazal-UR-Rehman, N. Ahmed, and M. U. Shehzad, "A robust H_∞ control for unmanned aerial vehicle against atmospheric turbulence," *2nd International Conference on Robotics and Artificial Intelligence (ICRAI)*, 2016, pp. 1-6.

Biographies



Madi Said obtained a master's degree in LMD in electro-mechanics in 2018 from El-Oued University, Algeria. He continues his PhD studies at the University of August 20, Skikda, Algeria, since 2019, specializing in electro-mechanics in the mechanical engineering laboratory. He is currently working in the education sector. His

research interests include control design in multiple systems, the uses, and applications of sensors, and electrical machines.

E-mail: s.madi@univ-skikda.dz



Mohand Said Larabi received his Engineer's Degree in Automatic control from the University of Skikda, Algeria in 2005, and his Master's Degree in Advanced Automatics from the University of Annaba, Algeria in 2008. He is currently a doctoral PhD in automatics at the University of Annaba, and an Assistant Teacher

/Researcher with the Department of Electrical Engineering at the University of Skikda, Algeria since 2014. And Associate researcher with the Automatic Laboratory of Skikda. His research interests are optimal control and robust control for multivariable systems.

E-mail: ms.larabi@univ-skikda.dz



Nacereddine Mohamed Kherief obtained a master's degree in 2007, then a doctorate in electromechanical engineering in 2013, and in 2017, he obtained a university qualification certificate. Since 1992 he has been a professor at the Normal High School of Technology Education (NHSTE), at the University of Skikda, Algeria. He is the

author of several International publications and scientific papers. He is also a team leader and member of several research projects. His studies focus on automatic, magnetohydrodynamics, control and modelling.

E-mail: kherief2009@yahoo.fr